

Structure, rotational dynamics, and superfluidity of small OCS-doped He clusters

Saverio Moroni,^{1,*} Antonio Sarsa,^{2,†} Stefano Fantoni,^{2,‡} Kevin E. Schmidt,^{2,§} and Stefano Baroni^{2,3,¶}

¹SMC INFM – Istituto Nazionale per la Fisica della Materia and Dipartimento di Fisica, Università di Roma La Sapienza
Piazzale Aldo Moro 2, I-00185 Rome, Italy

²SISSA and INFM DEMOCRITOS National Simulation Center
Via Beirut 2-4, I-34014 Trieste, Italy

³Chemistry Department, Princeton University, Princeton NJ 08544, USA

(Dated: December 11, 2002)

The structural and dynamical properties of OCS molecules solvated in Helium clusters are studied using reptation quantum Monte Carlo, for cluster sizes $n = 3 - 20$ He atoms. Computer simulations allow us to establish a relation between the rotational spectrum of the solvated molecule and the structure of the He solvent, and of both with the onset of superfluidity. Our results agree with a recent spectroscopic study of this system, and provide a more complex and detailed microscopic picture of this system than inferred from experiments.

PACS numbers: 36.40.-c, 61.46.+w, 67.40.Yv, 36.40.Mr, 02.70.Ss

Solvation of atoms and molecules in He nanodroplets provides a way to study their properties in an ultra-cold matrix, and also offers a unique opportunity to probe the physics of quantum fluids in confined geometries. Research in this field has been recently reviewed in Ref. [1], with emphasis on experiment and hydrodynamic modeling, and in Ref. [2], with emphasis on computer simulations.

Carbonyl sulfide (OCS) is one of the most widely studied dopants of He clusters (OCS@He _{n}) [3, 4], both because of its strong optical activity in the infrared and microwave spectral regions, and also because the OCS@He₁ complex is spectroscopically well characterized [5, 6], thus providing a solid benchmark for the atom-molecule interaction potential which is the key ingredient of any further theoretical investigation.

In the quest of fingerprints of superfluidity in the spectra of small- and intermediate-size He clusters, Tang *et al.* have recently determined the vibrational and rotational spectra of OCS@He _{n} at high resolution for $n = 2 - 8$ [3]. The main results of that investigation are: *i*) the rotational constant of the solvated molecule roughly equals the nanodroplet (large- n) limit [7] at $n = 5$, but then undershoots this asymptotic value up to the maximum cluster size ($n = 8$) attained in that work; *ii*) the centrifugal distortion constant has a minimum at $n = 5$, thus indicating that the complex is more rigid at this size; *iii*) the fundamental vibrational frequency of OCS is not a monotonic function of the number of He atoms, but it displays a maximum at $n = 5$, again suggesting a stronger rigidity at this size. Findings *ii*) and *iii*) suggest—and our study of the rotational spectra confirms—that $n = 5$ is a magic size related to the structure of solvent atoms around the solvated molecule. Finding *i*) implies the existence of a (yet to be determined) minimum in the rotational constant as a function of the cluster size. The occurrence of this minimum was interpreted as due to quantum exchanges which would decrease the effective inertia of the first solvation shell and would thus be a signature of the onset of *superfluidity* in this finite system [3].

Quantum simulations are complementary to the experiment for understanding the properties of matter at the atomic scale. In fact, while being limited by our incomplete knowledge of

the inter-atomic interactions and by the size of the systems one can afford to examine, simulations provide a wealth of detailed information which cannot be obtained in the laboratory. In this paper we show how state-of-the art quantum Monte Carlo simulations can be used to get an unparalleled insight into the exotic properties of small He clusters. At the same time, some of the dynamical properties thus predicted are so sensitive to the details of the atom-molecule interactions, to provide a very accurate test of the available model potentials.

The structure and the rotational dynamics of OCS@He _{n} clusters are studied here in the small-to-intermediate size regime ($n = 3 - 20$), using *reptation quantum Monte Carlo* (RQMC) [8], a technique by which ground-state properties (such as the density distribution and various static and dynamic correlations) can be determined with high accuracy. In particular, the analysis of the dynamical dipole correlation function allows us to resolve, for the first time theoretically, several rotational components of the spectrum of an interacting quantum system. RQMC combines the best features of the path-integral (PIMC) and diffusion quantum Monte Carlo (DQMC) techniques, yet avoiding some of their drawbacks: RQMC is not affected by the systematic errors which plague the estimate of ground-state expectation values in DQMC (the so called mixed-estimate and population-control biases) and gives easy access to time correlations, from which dynamical properties can be extracted [8]; at the same time, the RQMC technique is specially tailored to the zero-temperature (ground-state) regime, where PIMC becomes inefficient.

Both the He-He and the He-OCS interactions used here are derived from accurate quantum-chemical calculations [9, 10]. The OCS molecule is allowed to perform translational and rotational motions, but it is assumed to be rigid. The trial wavefunction is chosen to be of the Jastrow form: $\Phi_T = \exp \left[- \sum_{i=1}^n \mathcal{U}_1(r_i, \theta_i) - \sum_{i < j} \mathcal{U}_2(r_{ij}) \right]$, where r_{ij} is the distance between the i -th and the j -th helium atoms, $r_i = |\mathbf{r}_i|$ the distance of the i -th atom from the center of mass of the molecule, and θ_i is the angle between the molecular axis and \mathbf{r}_i . On account of the high anisotropy of the He-OCS poten-

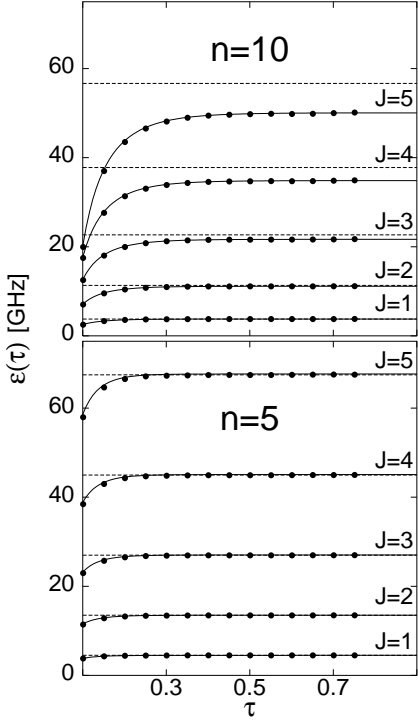


FIG. 1: Logarithm of the multipole correlation function, normalized by the spectral weight of the lowest-lying state: $\epsilon(\tau) = -\log(c_J(\tau)/A_J)/\tau$, for $n = 5$ (lower panel) and $n = 10$ (upper panel). Time units are ${}^\circ\text{K}^{-1}$.

tial, \mathcal{U}_1 is expanded as a sum of five products of radial functions times Legendre polynomials. All radial functions (including \mathcal{U}_2) are optimized independently for each cluster size with respect to a total of 27 variational parameters. The propagation time is set to $1 {}^\circ\text{K}^{-1}$, with a time step of $10^{-3} {}^\circ\text{K}^{-1}$. The effects of the length of the time step and of the projection time [8] have been estimated by test simulations performed by halving the former or doubling the latter. These effects were barely detectable on the total energy, and negligible with respect to the statistical noise for the properties on which we base our discussion below.

The absorption spectrum of a molecule solvated in a non polar environment is given by the Fourier transform of the autocorrelation function of its dipole, \mathbf{d} : $I(\omega) \propto 2\pi \sum_n |\langle \Psi_0 | \mathbf{d} | \Psi_n \rangle|^2 \delta(E_n - E_0 - \omega) = \int e^{i\omega t} \langle \mathbf{d}(t) \cdot \mathbf{d}(0) \rangle dt$, where Ψ_0 and Ψ_n are ground- and excited-state wavefunctions of the system respectively, E_0 and E_n the corresponding energies, and $\langle \cdot \rangle$ indicates ground-state expectation values. The dipole of a linear molecule—such as OCS—is oriented along its axis, so that the optical activity is essentially determined by the autocorrelation function of the molecular orientation vorsor: $c(t) = \langle \mathbf{n}(t) \cdot \mathbf{n}(0) \rangle$. Within RQMC the analytical continuation to imaginary time of this correlation function, $\bar{c}(\tau) = c(-i\tau)$, can be conveniently calculated without any other approximations than those implicit in the use of a given parametrization of the interatomic potentials [8]. From now on, when referring to *time correlation functions*, we will mean quantum correlations in imag-

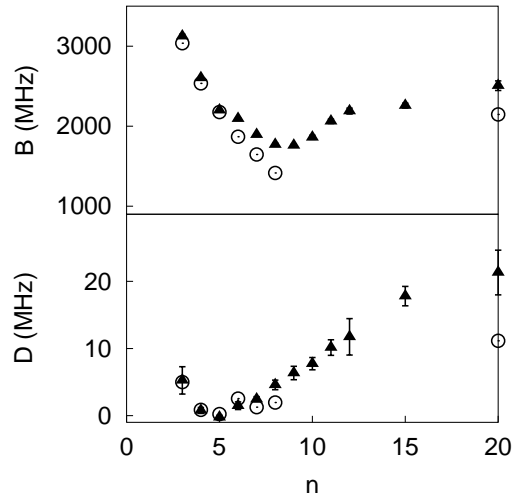


FIG. 2: Rotational constants (upper panel) and rotational distortion constant (lower panel, see text) of OCS@He_n, as functions of the cluster size, n . Triangles indicate the results of the present simulation, whereas circles are experimental data from Ref. [3].

inary time, and will we drop the bar over $\bar{c}(\tau)$. Analytical continuation to imaginary time transforms the oscillatory behavior of the real-time correlation function—which is responsible for the δ -like peaks in its Fourier transform—into a sum of decaying exponentials whose decay constants are the excitation energies, $E_n - E_0$, and whose spectral weights are proportional to the absorption oscillator strengths, $|\langle \Psi_0 | \mathbf{d} | \Psi_n \rangle|^2$. Dipole selection rules imply that only states with $J = 1$ can be optically excited from the ground state. Information on excited states with different angular momenta, J , can be easily extracted from the multipole correlation functions, $c_J(\tau)$, defined as the time correlations of the Legendre polynomials: $c_J(\tau) = \langle P_J(\mathbf{n}(\tau) \cdot \mathbf{n}(0)) \rangle \equiv \left\langle \frac{1}{2J+1} \sum_{M=-J}^J Y_{JM}^*(\mathbf{n}(\tau)) Y_{JM}(\mathbf{n}(0)) \right\rangle$. For each value of J , the value of the lowest-lying excitation energy, ϵ_J —i.e. the smallest decay constant in $c_J(\tau)$ —as well as the corresponding spectral weight, A_J , can be extracted from a fit to $c_J(\tau)$. We have verified that the values so obtained are rather insensitive to the details of the fitting procedure.

In Fig. 1 we display multipole correlations calculated up to $J = 5$ for OCS@He₅ and OCS@He₁₀. For a rigid-top, time correlations are described by a single exponential for each value of J , $c_J(\tau) = e^{-\epsilon_J \tau}$, whose decay constant is $\epsilon_J = BJ(J+1)$. The rigid-top energy levels are displayed as dashed lines. Time correlations deviate from a single-exponential behavior only at short times, thus indicating that the non rigidity of the cluster only affects the spectra at very high frequencies, the deviation being larger the larger the angular momentum. The dependence of ϵ on J is accurately predicted by the rigid-top model for $n = 5$, while it is less so for $n = 10$. In all cases the excitation energies are well described by a formula containing an effective centrifugal distortion constant: $\epsilon_J = BJ(J+1) - DJ^2(J+1)^2$ [12].

In Fig. 2 we display the rotational constant, B , and cen-

trifugal distortion constant, D , as functions of the cluster size. B displays a minimum at $n = 8 - 9$, while D is minimum at $n = 5$, indicating a greatest rigidity of the He@OCS complex at this size. In order to discuss these findings and their relation with the structure of the cluster, with the onset of superfluidity, and with the quality of the interaction potential used for the simulation, we first define $\rho(\mathbf{r})$ as the He number-density distribution, and $\phi(\mathbf{r})$ as the ground-state expectation value of molecule-atom angular motion correlation: $\phi(\mathbf{r}) = -\langle \Psi_0 | \mathbf{L} \cdot \mathbf{l}(\mathbf{r}) | \Psi_0 \rangle$. In this expression \mathbf{L} indicates the angular momentum of the OCS molecule and $\mathbf{l}(\mathbf{r})$ is the angular-current operator of He atoms at point \mathbf{r} : $\mathbf{l}(\mathbf{r}) = -i \hbar \mathbf{r} \times \sum_l \left(\frac{\partial}{\partial \mathbf{r}_l} \delta(\mathbf{r} - \mathbf{r}_l) + \delta(\mathbf{r} - \mathbf{r}_l) \frac{\partial}{\partial \mathbf{r}_l} \right)$. The angular correlation function, $\phi(\mathbf{r})$, is non-negative and it is large whenever the angular motion of He atoms at point \mathbf{r} is strongly correlated with the rotation of the solvated molecule, thus contributing to the molecular effective moment of inertia.

In Fig. 3 we display $\rho(\mathbf{r})$ and $\phi(\mathbf{r})$, as calculated for cluster sizes $n = 5, 8, 10, 15$. The He density reaches its maximum where the He-OCS interaction potential is minimum, *i.e.* in a *doughnut* surrounding the molecule perpendicular to the OC bond. This doughnut can accommodate up to 5 He atoms which rotate rather rigidly with the OCS molecule, as demonstrated by the large value of the angular correlation function. Each He atom within the doughnut gives a same contribution to the cluster moment of inertia, resulting in a constant slope of B vs. n for $n \leq 5$.

Secondary minima of the He-OCS potential exist on the molecular axis near the two poles, the one nearest to the S atom being deeper. For $n > 5$ He atoms spill out of the region of the main minimum and spread towards other regions of space, preferentially near the molecular poles. A detailed analysis of the He density plots for $n = 6, 7, 8$ shows that—due to quantum tunneling to and from the doughnut—both polar regions start to be populated as soon as the doughnut occupation is completed (*i.e.* for $n > 5$). The number of Helium atoms near the sulfur pole is 0.2, 0.3, and 0.7, for $n = 6, 7, 8$, and 0.5, 0.8, and 1.1 near the oxygen pole. Helium density is larger near the oxygen pole—rather than near sulfur where the potential is more attractive—because a smaller energy barrier and a smaller distance from the absolute minimum in the doughnut make quantum tunneling between the absolute and the secondary minima easier in this case.

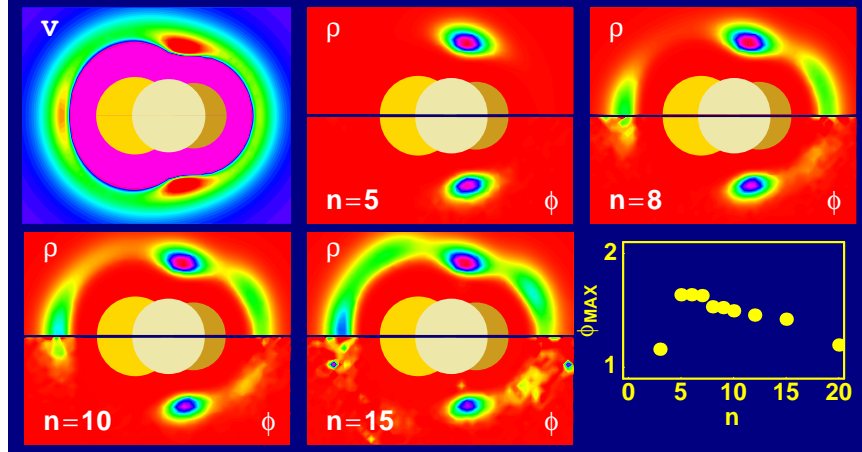
Quantum tunneling is the key for understanding the onset of superfluidity, as well as the sensitivity of rotational spectra to the details of the He-OCS interaction. For $n = 6, 7, 8$ a sizeable He density is found not only near the molecular poles, but also in the angular region between the doughnut and the oxygen pole, where the energy barrier is small. Non negligible angular correlations indicate that atoms in this region (and not only near the poles) contribute to the effective moment of inertia. For $n > 8$ He atoms start to fill the angular region between the doughnut and the S pole (see the $n = 10$ panel of Fig. 3). The closure of He rings in the sagittal planes makes atomic exchanges along these rings possible, thus triggering

the same mechanism which gives rise to superfluidity in infinite systems [11]. The onset of superfluidity is responsible not only for negligible angular correlations in this region, but also for the decrease of these correlations in the doughnut region where the largest contributions to the cluster inertia come from. This is demonstrated in the bottom-right panel of Fig. 3, where one sees that the maximum of the angular correlation in the doughnut region starts decreasing for $n > 8$.

It is also interesting to examine the dependence upon cluster size of the spectral weights, A_J . It turns out that, while for $J = 1$ the spectral weight displays a maximum at $n = 4 - 5$ and a minimum at $n = 8$, the maximum at $n = 4 - 5$ is not followed by any minimum for $J = 5$. We interpret the maximum of A_J at $n = 4 - 5$ as another manifestation of the greatest rigidity of the He@OCS cluster at this size, while the behavior for $n > 5$ is determined by the number of solvent states available to couple with the lowest-lying molecular rotation. This number increases with the cluster size for $J = 5$, while it has a maximum at $n = 8 - 9$ for $J = 1$. These findings are consistent with the emergence of superfluid behavior at cluster size, as characterized by the reduction of low-lying excited states in the He matrix [11].

This quantum tunneling makes the rotational constants for $n > 5$ rather sensitive to the height and width of the barriers between different minima of the OCS-He interaction potential. On the other hand, the details of the potential off the main minimum in the doughnut hardly affect the spectra for $n \leq 5$ and, in particular, that of OCS@He₁ which is used as a benchmark for the quality of the potential [10]. Our simulations predict rotational constants which are in excellent agreement with experiment for $n \leq 5$, while for $n \geq 6$ the predicted values of B are too large and display too small a slope as a function of n . We believe that both these facts are due to the smallness of the barriers between the main and the secondary energy minima, which determines an excessive spill-out of He atoms off the main minimum for $n = 6$ and an excessive propensity towards atomic exchanges for $n \geq 6$. We expect that larger energy barriers would result in a better agreement between theory and experiment for $6 \leq n \leq 8$ and, possibly, in a shift of the predicted minimum of the rotational constant towards larger sizes. As a qualitative test, we have redone some of our simulations with a uniformly scaled potential ($V_{\text{He-OCS}} \rightarrow \alpha V_{\text{He-OCS}}$). Although not very realistic, this transformation captures the essential modifications to be done to the potential, *i.e.* it modifies the height of the barriers while leaving the location of the minima unchanged. For $\alpha = 1.2$, we find that the values of B for $n \leq 5$ are left practically unchanged, while the agreement with experiment is much improved for $n = 6, 7, 8$. The resulting minimum value of B stays located near $n = 8 - 9$. This lets us believe that our prediction of the position of the minimum rotational constant as a function of the cluster size should be rather robust with respect to possible improvements of the He-OCS effective potential.

FIG. 3: Upper left panel: He-OCS interaction potential. The atoms constituting the molecule are displayed as circles whose radius is the corresponding Van der Waals radius (sulphur on the left). Panels with red background: upper mid panel, He number density; lower mid panel, angular motion correlation function (see text). Colors go from red to violet as in a rainbow, as the value of the function increases. Lower right panel: maximum of the angular motion correlation function, as a function of the cluster size.



In conclusion, we have shown that state-of-the art quantum Monte Carlo simulation provide both a qualitative explanation of the relation existing among structure, dynamics, and superfluidity in small He clusters, and a sensitive test of the quality of atom-molecule potentials, in regions which hardly affect the spectra of the monoatomic molecular complex.

We are grateful to W. Jäger for sending us a preprint of Ref. [3] prior to publication, and to G. Scoles for bringing that paper to our attention and for a careful reading of the first draft of the present paper. Last but not least, we would like to thank both K. Lehman and G. Scoles for many illuminating discussions held at the Chemistry Department of the Princeton University where SB was the grateful guest of R. Car while part of this work was being done.

J. Chem. Phys. **113**, 6469 (2000).
[3] J. Tang, Y. Xu, A. R. W. McKellar, and W. Jäger, Science, in press.
[4] F. Paesani, F. A. Gianturco, and K. B. Whaley, J. Chem. Phys. **115**, 10225 (2001); F. Paesani, A. Viel, F. A. Gianturco, and K. B. Whaley, unpublished.
[5] K. Higgins and W. Klemperer, J. Chem. Phys. **110**, 10225 (2001).
[6] J. Tang and A. R. W. McKellar, J. Chem. Phys. **115**, 3053 (2001).
[7] S. Grebenev, J. P. Toennies and A. F. Vilesov, Science **279** 2083 (1998).
[8] S. Baroni and S. Moroni, Phys. Rev. Lett. **82**, 4745 (1999); a pedagogical introduction to the method can be found in: S. Baroni and S. Moroni, in *Quantum Monte Carlo Methods in Physics and Chemistry*, edited by P. Nightingale and C.J. Umrigar. NATO ASI Series, Series C, Mathematical and Physical Sciences, Vol. 525, (Kluwer Academic Publishers, Boston, 1999), p. 313 (see also: <http://xxx.lanl.gov/abs/cond-mat/9808213>).
[9] T. Korona, H. L. Williams, R. Bukowski, B. Jeziorski and K. Szalewicz, J. Chem. Phys. **106**, 5109 (1997).
[10] J. M. M. Howson and J. M. Hutson J. Chem. Phys. **115**, 5059 (2001).
[11] R. P. Feynman, Phys. Rev. **91**, 1291 (1953); *ibid.*, p. 1301.
[12] The evaluation of the distortion constant, D , is much facilitated by the fact that large correlations exist among the time series from which values of $c_J(\tau)$ are extracted for different values of J (they all derive from a same underlying random walk). Because of this, the statistical error in the ratio of any two c_J 's (whose logarithmic derivatives gives excitation energies) is smaller than the error on individual c_J 's.

* Electronic address: moroni@caspur.it

† Electronic address: sarsa@sissa.it; Present address: Departamento de Fisica Moderna, Universidad de Granada, E-18071 Granada, Spain.

‡ Electronic address: fantoni@sissa.it

§ Electronic address: Kevin.Schmidt@asu.edu; Permanent address: Department of Physics and Astronomy, Arizona State University, Tempe, Arizona 85287.

¶ Electronic address: baroni@sissa.it; Permanent address: SISSA and DEMOCRITOS, Trieste, Italy.

[1] C. Callegari, K. K. Lehmann, R. Schmied and G. Scoles, J. Chem. Phys. **115**, 10090 (2001).
[2] Y. Kwon, P. Huang, M. V. Patel, D. Blume and K. B. Whaley,